
Toward Cost-effective Control of Wall Turbulence for Skin Friction Drag Reduction

¹Nobuhide Kasagi, ¹Yosuke Hasegawa, and ²Koji Fukagata

¹Department of Mechanical Engineering, The University of Tokyo, Hongo 7-3-1, Bunkyo-ku, Tokyo 113-8656, Japan

²Department of Mechanical Engineering, Faculty of Science and Technology, Keio University, Hoyoshi 3-14-1, Kohoku-ku, Yokohama 223-8522, Japan
kasagi@tthtlab.t.u-tokyo.ac.jp

Abstract

This paper discusses the active control of turbulence for skin friction reduction with an emphasis on cost effectiveness. By introducing performance indices such as the net energy saving rate and the control gain, we assess existing control algorithms for true energy saving. We review recent attempts to reduce costs accompanying practical applications, and discuss remaining issues in developing more practically applicable control algorithms.

1 Introduction

Facing the global issues such as depletion of energy resources and environmental deterioration, highly advanced technology of turbulence control is ever more needed. Turbulence control opens up new possibilities to achieve far greater efficiency and least environmental impact of various thermal-fluid systems supporting the human society through the manipulation and modification of momentum/heat/mass transfer, noise as well as chemical reaction.

In this paper, we focus on the turbulent flow control for skin friction drag reduction. During the past several decades, an enormous amount of time and effort of the turbulence research community has been devoted to advance the understanding of dynamical mechanism of the near-wall coherent structures, and this has been accomplished by exploiting modern measurement techniques and computational fluid dynamics. For example, it is now well known that large skin frictional drag in turbulent flow is attributed to the existence of near-wall vortical structures and associated ejection/sweep events (Robinson, 1991; Hamilton et al., 1995). Based on this knowledge, various flow control strategies have been proposed, although most of them are tested and evaluated simply in terms of the drag reduction rate. However, the time has come for

us to make assessment of any new control method by taking into account the total cost of manufacturing, installation, operation and maintenance, and we should aim at developing such control as to achieve high cost-effectiveness even in fundamental research work.

Existing control schemes are roughly classified into two categories, i.e., active and passive controls. Passive control as typified by a riblet surface has an advantage that it does not need continuous power supply to sustain the flow control. However, the control performance achieved is generally worse if compared to active control. In addition, the effectiveness of passive control is often limited under flow conditions close to a design point. Development of robust and effective passive control schemes is still a challenging issue.

Active control is further classified into predetermined and feedback controls. In the former, its control input is specified *a priori* as in spanwise wall-oscillation (Jung et al., 1992; Quadrio and Ricco, 2004), streamwise/spanwise traveling waves (Min et al., 2006; Du et al., 2002), and steady streamwise forcing (Xu et al., 2007) without knowing a turbulence state at each instant. Existing predetermined controls commonly suffer from a disadvantage of large power consumption as will be discussed later. On the contrary, in a feedback control its input is always determined from sensor signals by a control law, so that it can be more robust and flexible.

The feedback control generally offers better control performance with smaller power consumption than the predetermined control. The former, however, has a disadvantage of requiring numerous sensors to detect an instantaneous flow state, of which signals are used to trigger actuators. In addition, measurable flow quantities are likely to be limited to those at the wall, where sensors can be implemented without changing the system design drastically. Most feedback control algorithms so far proposed assume that massively arrayed sensors and actuators are provided on a wall surface. Considering a fact that physical dimensions and response times of these hardware components should be very small, i.e., less than millimeter and millisecond (Kasagi et al., 2009), fabrication and maintenance of these devices would impose an unbearable cost even with rapidly developing MEMS technology. Thus, the predetermined control is superior in a sense that it employs a much simpler hardware system than the feedback control.

In the following, we will discuss several control schemes that are deemed to reduce incurring costs associated with predetermined and feedback controls. First, we introduce three kinds of indices to be considered in assessing the control and some fundamental theories on drag reduction. Then, we will review recent attempts to reduce various costs accompanying practical applications with a particular focus on control algorithm. For the recent progress of hardware components, refer to a review paper by Kasagi et al. (2009) and references therein.

2 Fundamental Concepts

2.1 Control Performance Indices

Consider a constant-rate flow driven by a pressure gradient in a straight duct, where the form drag is zero. Then, the pressure gradient must be balanced with the total skin friction at the wall. Obviously, the drag reduction rate R is equivalent to the reduction of pumping power P :

$$R = (P_0 - P)/P_0 \quad (1)$$

where the subscript of 0 represents a quantity in the original uncontrolled flow. By taking into account the power consumption P_{in} to manipulate the flow, the net energy saving rate S is defined as:

$$S = \{P_0 - (P + P_{in})\}/P_0. \quad (2)$$

Another important parameter is the effectiveness of a control algorithm, i.e., the gain G defined as:

$$G = (P_0 - P)/P_{in}, \quad (3)$$

which is the reduction of pumping power divided by the control power input.

The above three parameters are related as follows.

$$S = R(1 - G^{-1}). \quad (4)$$

Presently, we choose S and G as performance indices for evaluating a control algorithm, although there are also the practical cases where only direct control effect is of interest from a viewpoint of merits such as utmost speed of cruising, least level of noise and/or extremely high rates of heat transfer and combustion. The index of S represents the maximum energy saving rate achieved when neglecting all possible energy losses in driving hardware components. Obviously, in order to obtain a net energy saving, i.e., $S > 0$, G need to be larger than 1. In a real system, however, there always exist such energy losses associated with actuators, sensors, control circuits and so forth. Hence, in order to achieve a true energy saving in a real system, G should be sufficiently large regardless of R . For instance, when G is 10, the overall hardware efficiency should be much higher than 10 % in order to have $S \gg 0$.

In Fig. 1, typical data of S and G obtained by active control schemes are plotted. Here, all results are obtained in fully developed turbulent channel flow at relatively low friction-based Reynolds numbers from $Re_\tau = 110$ to 640. Since S and G strongly depend on parameters in each control scheme, we select only favorable results in this figure. These include: feedback controls such as V-control (Choi et al., 1994) and suboptimal control (Lee et al., 1998) assessed at different Reynolds numbers by Iwamoto et al. (2002), temporally-periodic spanwise wall-oscillation control (Quadrio and Ricco, 2004), streamwise traveling wave control (Min et al., 2006), steady streamwise forcing control (Xu et

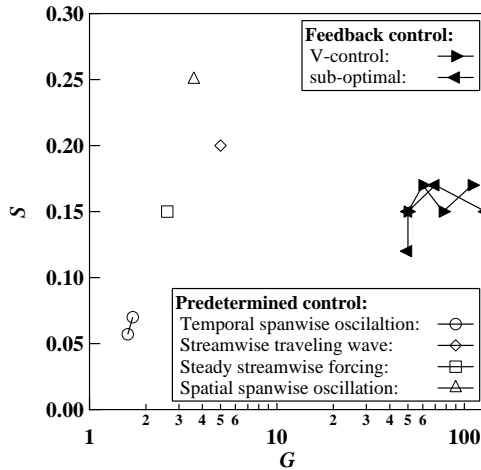


Fig. 1. Net energy saving rate achieved by different active control schemes: V-control and suboptimal control (Iwamoto et al., 2002), temporally-periodic spanwise wall-oscillation control (Quadrio and Ricco, 2004), streamwise traveling wave control (Min et al., 2006), steady streamwise forcing control (Xu et al., 2007), and spatially-periodic spanwise oscillation control (Yakeno et al., 2009).

al., 2007) and spatially-periodic spanwise oscillation control (Yakeno, et al., 2009). Other predetermined controls such as spanwise traveling wave control (Du et al., 2002) and large-scale streamwise vortex excitation control (Schoppa and Hussain, 1998) are not included since their control power inputs are not known.

It is found that the net energy saving rate S achieved by the predetermined controls can be comparable or even better compared to the feedback controls. Once G is considered, however, one can see that the values of the predetermined controls are at most $G \sim 5$ and generally much smaller, say, by one or two orders of magnitude, than those achieved by the feedback controls. For example, the maximum gain $G = 1.7$ achieved by the temporally periodic spanwise wall-oscillation makes S reach its maximum of 7%. In this case, the actuator efficiency must be larger than $1/G \sim 60\%$ in order to obtain net energy saving. This is not easy generally, and should impose a severe constraint in practical applications.

2.2 Theoretical Constraint

Drag reduction rate

Fukagata et al. (2002) derived a simple mathematical relationship between the skin friction coefficient and the Reynolds stress distribution from the streamwise momentum equation. In the case of a fully developed channel flow, the result leads to:

$$C_f = \frac{12}{Re_b} + 12 \int_0^1 2(1-y)(-\overline{u'v'})dy, \quad (5)$$

where $y = 0$ and 1 correspond to the wall and the channel center, respectively, and the overbar denotes the average in homogeneous directions. All the variables are made dimensionless by using the channel half-width and twice the bulk mean velocity, and Re_b denotes the bulk Reynolds number. The above identity indicates that the skin friction coefficient is decomposed into the laminar contribution, $12/Re_b$, which is identical to the well-known laminar solution, and the turbulent contribution, which is proportional to the weighted spatial average of Reynolds stress. Note that the weight linearly decreases with the distance from the wall.

The identity suggests that sublaminal friction drag, which is smaller than that of the laminar flow at the same flow rate, is attained if the second term on the RHS of Eq. (5) becomes negative. Actually, Fukagata et al. (2005) and Min et al. (2006) have achieved sublaminal drag by applying a virtual body force in the wall-normal direction and a traveling wave-like blowing/suction, respectively. This is only possible with a penalty of $S < 0$ as described below.

Lower-bound for minimum energy consumption

It is mathematically proved that there exists a lower bound for the minimum energy consumption in any skin friction control (Fukagata et al., 2009; Bewley, 2009). In a fully developed channel flow, the sum of pumping and control work should be eventually dissipated by viscosity. Hence, minimizing the total power is equivalent to minimizing the volume integral of the viscous dissipation over the whole flow domain. Under a constant mass flow rate and a no-slip condition at top and bottom walls, it can be proved that the laminar velocity profile gives the minimum viscous dissipation, and therefore the minimum power input. This fact indicates that the ultimate goal of skin friction drag reduction control for energy saving is to lead the turbulent flow toward a relaminarized state.

2.3 Toward Control of High Reynolds Number Flows

In real applications, the Reynolds number is far beyond the values that DNS can reach, whilst various flow control strategies have been tested in relatively simple canonical flows at low Reynolds numbers. Assessment of V-control and suboptimal control in fully developed channel flow by Iwamoto et al. (2002) demonstrated that the degree of drag reduction gradually decreases with increasing the Reynolds number from $Re_\tau = 110$ to 640. A similar trend is also observed for spanwise wall-oscillation control (Choi et al., 2002; Ricco and Quadrio, 2008).

Figure 2 shows the weighted Reynolds shear stress, $(1 - y)(-\overline{u'v'})$, i.e., the integrand of the second term in Eq. (5), in uncontrolled flows at different Reynolds numbers. At higher Reynolds numbers, the relative contribution of the near-wall Reynolds shear stress to the friction drag drastically decreases, whereas that of the outer layer becomes dominant. Therefore, a

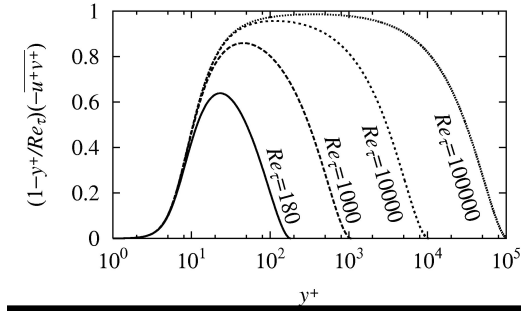


Fig. 2. Weighted Reynolds shear stress at different Reynolds numbers calculated from the eddy viscosity model with the van Driest damping function (Kasagi et al., 2009).

question arises whether the conventional near-wall manipulation is effective even at high Reynolds numbers.

Iwamoto et al. (2005) numerically simulated a fully developed turbulent channel flow with damping of velocity fluctuations in the near-wall layer and derived a theoretical relationship among the Reynolds number Re_τ of uncontrolled flow, the damping layer thickness y_d/δ non-dimensionalized by the channel half width δ and the drag reduction rate R . As a result, they found that the dependency of R on Re_τ is moderate. For instance, when the fluctuation at $y_d^+ < 10$ is damped, R is about 43 % at $Re_\tau = 10^3$, while 35 % even at $Re_\tau = 10^5$, where the damping layer is extremely thin compared to the channel half-width, i.e., $y_d/\delta = 10^{-4}$.

The reason for the success of near-wall manipulation is explained as follows. The velocity inside the thin damping layer, which is increased as a result of turbulence damping by the control, results in the decreased velocity difference between the outer edge of the damping layer and the channel center. Therefore, the effective Reynolds number of the bulk flow is much reduced. This example suggests that the basic strategy of attenuating only near-wall turbulence can be considered valid even when the Reynolds number is considerably increased.

3 Feedback Control

3.1 Control Algorithms with Wall Sensors

In real systems, the available state information is considered to be practically limited to the following quantities: (1) the streamwise wall-shear stress, $\tau_{wx} = (\mu \partial u / \partial y)_w$; (2) the wall pressure, p_w ; and (3) the spanwise wall-shear stress, $\tau_{wz} = (\mu \partial w / \partial y)_w$. According to DNS studies, the control algorithms using τ_{wz} or p_w are very effective (Lee et al., 1997; Lee et al., 1998; Koumoutsakos, 1999). These quantities, however, are in most cases difficult to measure by using small sensors distributed on the wall (Kasagi et al., 2009).

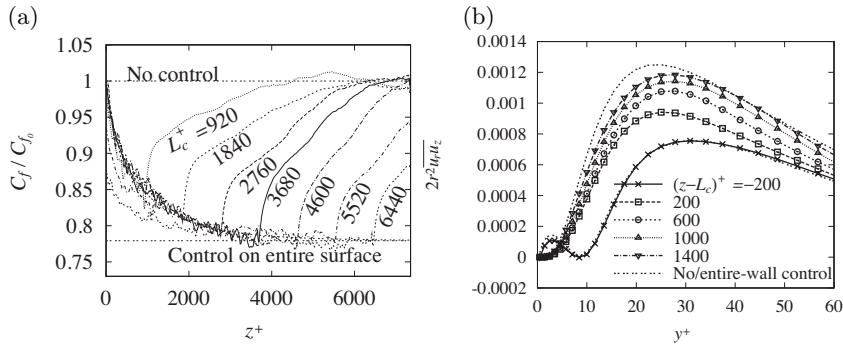


Fig. 3. DNS results of turbulent pipe flow with the opposition control applied to a partial area (Fukagata and Kasagi, 2003): (a) Normalized local skin friction coefficient as a function of streamwise location, for different control lengths, L_c , (b) Profiles of Reynolds shear stress weighted by $2r^2$ (in accordance with the FIK identity for pipe flows) around the termination point of control.

Development of effective control algorithms based on τ_{wx} was initially judged difficult. For example, Lee et al. (1998) succeeded in τ_{wz} - and p_w -based suboptimal schemes, but they failed to reduce the drag by sensing only τ_{wx} . A reason for this failure may be attributed to their cost function based on the fluctuating wall shear stress $(\tau'_{wx})^2$, of which relationship to the mean shear is not always clear. In fact, Fukagata and Kasagi (2004) redefined the cost function based on the near-wall Reynolds shear stress, which is directly related to the friction drag like in Eq. (5). They successfully attained 11% drag reduction in their DNS of turbulent pipe flow.

Control algorithms using τ_{wx} has also been developed by the physical argument or by adopting evolutionary optimization techniques. Based on the correlation between the near-wall structure and wall variables, Endo et al. (2000) proposed an algorithm to attenuate the meandering of low-speed streaks. Morimoto et al. (2002) used a genetic algorithm (GA) to optimize weights in a prescribed function, which determined actuator's movement from sensor signals. About 10% drag reduction was attained in both cases. Yoshino et al. (2008) also used a GA in their MEMS-based feedback control system in a wind-tunnel experiment and obtained about 6% drag reduction. Recently, Frohnafel et al. (2009) proposed a new feedback control of attenuating the spanwise velocity fluctuation based on τ_{wx} measured upstream, and obtained almost 20 % drag reduction, which is the highest value achieved by sensing τ_{wx} only.

3.2 Power Saving with Selective Space/Scale Control

Early studies of feedback control always assumed control inputs ideally applied on the entire wall surface. From both technologically and economical

viewpoints, however, such design of a broad surface covered with an array of feedback control units is not feasible. Therefore, one may envision a control, of which effect would last over a long downstream distance, so that the cost can be reduced with simplified design and implementation.

Fukagata and Kasagi (2003) applied, in their DNS of pipe flow, the opposition control of Choi et al. (1994) only in the region of $0 < z < L_c$, while uncontrolling the rest of the region, $L_c < z < L$, where L is the computational domain length. Their results reveal that the drag reduction rate is nearly proportional to the ratio of controlled to total areas. This is attributed to the relatively fast recovery of the skin friction coefficient after the termination of control, as shown in Fig. 3(a). Similar results are reported by Pamiès et al. (2007) for a spatially-developing boundary layer under opposition control. As shown in Fig. 3(b), the quick recovery of local friction is caused by the quick response of Reynolds shear stress near the wall.

One may be able to save the control cost by limiting the scales of turbulence or number of modes. Suppose we can design a friction drag reduction technique to only manipulate large structures, it would be tremendously beneficial in terms of hardware development, particularly in higher Reynolds number flows; it would certainly relax various requirements for the size, dynamic range and frequency response of sensors and actuators.

Fukagata et al. (2008) explored such a possibility by means of DNS at $Re_\tau = 640$. As an idealized feedback control, they selectively damp either the small-scale wall-normal velocity fluctuations (defined as those with spanwise wavelengths smaller than 300 wall units) or the large-scale fluctuations (spanwise wavelengths larger than 300 wall units). They report that the damping of small-scale fluctuations is more efficient than that of large-scale ones as shown in Fig. 4, where the contributions of laminar and two different-scale Reynolds stress components to the skin friction under the selective scale controls are compared. When only the small ones are damped, the friction drag diminishes simply because of the absence of small-scale fluctuations near the wall. On the other hand, with the large-scale damping, the small-scale fluctuations are drastically increased and this results in the friction drag larger than expected from the absence of large-scale contributions.

From the studies above, it is conjectured that saving of control effort in space or scales is, in principle, difficult as far as the drag reduction relies on the suppression of fine-scale turbulence in the vicinity of the wall, although further study is needed for inventing new types of control.

4 Predetermined Control

Most predetermined controls employ a wall velocity, which has a spatial or temporal periodicity. These control inputs can be generally represented as:

$$u_i(x, 0, z, t) = \hat{u}_i \cdot \text{Real}[\exp\{i(\omega t + k_x x + k_z z)\}] \quad (6)$$

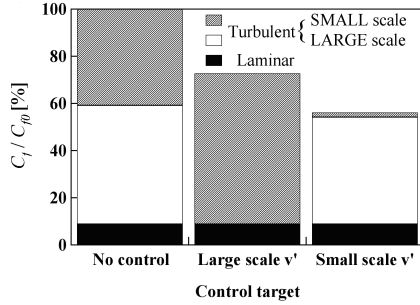


Fig. 4. Integral contributions to friction drag from different scales in DNS of channel flow at $Re_\tau = 640$ under idealized damping of wall-normal velocity fluctuations (Fukagata et al., 2008): Comparison between no-control, damping of large-scale only, and damping of small-scale only.

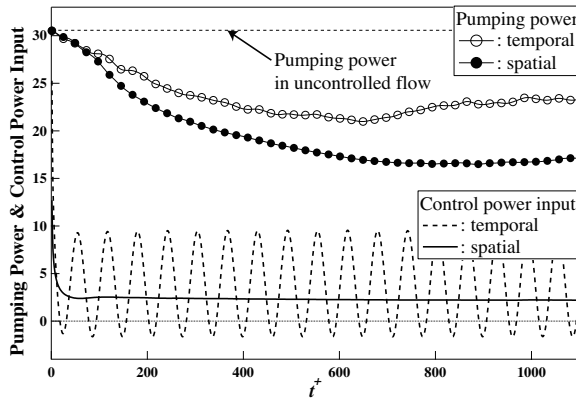


Fig. 5. Time traces of pumping and control power inputs under temporally- and spatially-periodic spanwise oscillation controls (Yakeno et al., 2009).

For example, the temporally-periodic spanwise (wall) oscillation control proposed by Jung et al. (1992) corresponds to $(\omega \neq 0, k_x = k_z = 0)$, while the traveling-wave controls such as Du et al. (2002) and Min et al. (2006) are defined as $(\omega \neq 0, k_z \neq 0)$ and $(\omega \neq 0, k_x \neq 0)$, respectively. Recently, stationary, but longitudinally-periodic controls, i.e., $(k_x \neq 0, \omega = k_z = 0)$, have been proposed by Quadrio et al. (2007) and Yakeno et al. (2009).

When such periodic wall velocity is assumed, the resultant velocity field would be a superposition of periodic and irregular components. Hence, by decomposing an instantaneous velocity u_i into a spatio-temporal mean component \bar{u}_i , a phase-fluctuating component \tilde{u}_i and a random incoherent component u_i'' , the Reynolds stress in the integrand of Eq. (5) can be rewritten as:

$$-\overline{u'v'} = -(\overline{\tilde{u}\tilde{v}} + \overline{u''v''}). \quad (7)$$

According to Eqs. (5) and (7), there are two possibilities to obtain drag reduction. The first strategy is to make the first coherent term negative, which is otherwise very small or almost zero. This strategy was successfully adopted by a traveling wave-type control by Min et al. (2006). The steady streamwise forcing by Xu et al. (2007) also applies a body force so as to directly reduce the

drag, namely, decelerating the flow in the near-wall layer, while accelerating further away from the wall.

The second strategy is to suppress the second incoherent term of Eq. (7), which is a major factor for skin friction drag in uncontrolled flow. For example, Yakeno et al. (2009) investigate the effects of two different spanwise wall velocities, which are temporally and spatially periodic, on the coherent structures and the resultant drag reduction. The temporally-periodic control is essentially the same as that proposed by Jung et al. (1992). In the spatially-periodic control, stationary, but longitudinally-periodic spanwise control input is applied at the wall. They show that there exist the optimal conditions for the period of $T^+ \sim 100$ and the streamwise wavelength $\lambda_x^+ \sim 1000$ for drag reduction. Time traces of the pumping and control power inputs under these conditions are shown in Fig. 5. The spatially-periodic control achieves larger drag reduction rate with less control power input, and gives larger net energy saving. In these cases, a drastic decrease in $-\overline{u''v''}$ accounts for the drag reduction.

Since the first term in Eq. (7) is a direct result of the introduced control input, so that it is easier to modify, the former strategy seems more feasible. However, the results of Min et al. (2006) and Xu et al. (2007) indicate that the second term in Eq. (7) is also decreased with their controls. Recently, the authors have tested control inputs, which force the first term to be negative at least in the very vicinity of the wall. In most cases, however, the drag increases against our expectation because of marked enhancement of the second term further away from the wall. These results suggest that modifying the random component $-\overline{u''v''}$ is primarily important for drag reduction.

The mechanism of turbulence suppression in the predetermined control has not been fully understood despite its simplicity. In contrast to the feedback control, where a control input is given so as to locally diminish a coherent streamwise vortex, the predetermined control is likely to prevent vortex generation by interfering the regeneration cycle near the wall (Hamilton et al., 1995). For example, the phase-averaged flow field around a streamwise vortex shown by Choi et al. (2002) clearly shows that the spanwise wall-oscillation control disrupts phase-locking of the streaks and streamwise vortices near the wall. Recently, Jovanović (2008) showed that the turbulence suppression due to spanwise wall-oscillation can be predicted by the receptivity analysis of the linearized Navier-Stokes equation. In contrast, Lee et al. (2008) conclude that a linear stability analysis of a channel flow subject to traveling wave-like blowing/suction from the wall cannot explain turbulence suppression observed in the corresponding DNS of Min et al. (2006). At this moment, it is not clear whether such stability analyses provide a unified explanation to turbulence suppression observed in various predetermined controls.

5 Conclusions and Challenges for the Future

We have briefly reviewed the recent advances in active turbulence control algorithms, particularly for skin friction drag reduction. With deepening understanding of the dynamical mechanism of near-wall coherent structures, various control strategies have been proposed by exploiting modern control theory, physical arguments, adaptive methods and so forth. Although most of them are validated under idealistic conditions, it is of great importance to assess any control method by taking into account the total cost of manufacturing, installation, operation and maintenance. Namely, we should pay much attention upon cost effectiveness even when developing a fundamental control law. From this viewpoint, the control gain should be much larger than unity to compensate possible energy losses in hardware components.

Feedback control generally works better than predetermined control in terms of the gain, since the former determines best control input by sensing the flow state at each time instant. In order to avoid a heavy burden associated with hardware requirements, however, it is desirable to develop a control algorithm that demands a reduced number of sensors and actuators. So far, reducing the surface control area has simply led to deteriorated overall control effectiveness, but selective wavenumber control should be worth further studying, particularly from a viewpoint of receptivity of the near-wall layer.

Predetermined control methods achieve considerable drag reduction with an advantage of easier implementation, but they are likely to suffer from large power consumption. This is a major problem in existing predetermined controls. Thus, it is strongly desired to minimize the control input while keeping its high control effectiveness. For this, understanding the mechanism of turbulence suppression due to a prescribed forcing mode should be indispensable.

So far, the control performance has been assessed at low Reynolds numbers. A few previous studies show that the drag reduction rate in both feedback and predetermined controls commonly tends to decrease gradually, although moderate, with increasing the Reynolds number. Applicability of these control strategies to practically high Reynolds number flows need to be further studied theoretically, numerically and experimentally.

With all above said, for real application of turbulence control technology, a breakthrough should be indispensable in design, fabrication and implementation of hardware components such as durable high-performance sensors, actuators and controllers (Kasagi et al., 2009).

Acknowledgements

This work was financially supported through the Grant-in-Aid for Scientific Research (A) (No. 20246036) by the Ministry of Education, Culture, Sports, Science and Technology (MEXT).

References

1. T. R. Bewley, *J. Fluid Mech.*, in press
2. H. Choi, P. Moin and J. Kim, *J. Fluid Mech.*, **262**, 75 (1994)
3. J. I. Choi, C. W. Xu and H. J. Sung, *AIAA Journal*, **40**, 842 (2002)
4. Y. Du, V. Simeonidis and G. E. Karniadakis, *J. Fluid Mech.*, **457**, 1 (2002)
5. T. Endo, N. Kasagi and Y. Suzuki, *Int. J. Heat Fluid Flow*, **21**, 568 (2000)
6. B. Frohnapfel, Y. Hasegawa and N. Kasagi, Proc. 6th Int. Symp. on Turbulence and Shear Flow Phenomena (TSFP6), Seoul, to be presented (2009)
7. K. Fukagata, K. Iwamoto and N. Kasagi, *Phys. Fluids*, **14**, L73 (2002)
8. K. Fukagata and N. Kasagi, *Int. J. Heat Fluid Flow*, **24**, 480 (2003)
9. K. Fukagata and N. Kasagi, *Int. J. Heat Fluid Flow*, **25**, 341 (2004)
10. K. Fukagata, N. Kasagi and K. Sugiyama, Proc. 6th Symp. Smart Control of Turbulence, Tokyo, 143 (2005)
11. K. Fukagata, M. Kobayashi, N. Kasagi, Proc. 7th Int. Symp. on Engineering Turbulence Modelling and Measurement (ETMM7), Cyprus, 131 (2008)
12. K. Fukagata, K. Sugiyama and N. Kasagi, *Physica D*, in press
13. J. M. Hamilton, J. Kim and F. Waleffe, *J. Fluid Mech.*, **287**, 317 (1995)
14. K. Iwamoto, Y. Suzuki and N. Kasagi, *Int. J. Heat Fluid Flow*, **23**, 678 (2002)
15. K. Iwamoto, K. Fukagata, N. Kasagi and Y. Suzuki, *Phys. Fluids*, **17**, 011702 (2005)
16. M. R. Jovanović, *Phys. Fluids*, **20**, 014101 (2008)
17. W. J. Jung, N. Mangiavacchi and R. Akhavan, *Phys. Fluids*, **4**, 1605 (1992)
18. N. Kasagi, Y. Suzuki and K. Fukagata, *Annu. Rev. Fluid Mech.*, **41**, 231 (2009)
19. P. Koumoutsakos, *Phys. Fluids*, **11**, 248 (1999)
20. C. Lee, J. Kim, D. Babcock and R. Goodman, *Phys. Fluids*, **9**, 1740 (1997)
21. C. Lee, J. Kim and H. Choi, *J. Fluid Mech.*, **358**, 245 (1998)
22. C. Lee, T. Min and J. Kim, *Phys. Fluids*, **20**, 101513 (2008)
23. T. Min, S. M. Kang, J. L. Speyer and J. Kim, *J. Fluid Mech.* **558**, 309 (2006)
24. K. Morimoto, K. Iwamoto, Y. Suzuki and N. Kasagi, Proc. 3rd Symp. Smart Control of Turbulence, Tokyo, 107 (2002)
25. M. Pamiès, E. Garnier, A. Merlenm and P. Sagaut, *Phys. Fluids* **19**, 108102 (2007)
26. M. Quadrio and P. Ricco, *J. Fluid Mech.*, **521**, 251 (2004)
27. M. Quadrio, J. M. Floryan and P. Luchini, *J. Fluid Mech.*, **576**, 425 (2007)
28. P. Ricco and M. Quadrio, *Int. J. Heat Fluid Flow*, **29**, 891 (2008)
29. S. K. Robinson, *Annu. Rev. Fluid Mech.*, **23**, 601 (1991)
30. W. Schoppa and F. Hussain, *Phys. Fluids*, **10**, 1049 (1998)
31. J. Xu, S. Dong, M. Maxey and G. E. Karniadakis, *J. Fluid Mech.*, **582**, 79 (2007)
32. A. Yakeno, Y. Hasegawa and N. Kasagi, Proc. 6th Int. Symp. on Turbulence and Shear Flow Phenomena (TSFP6), Seoul, to be presented (2009)
33. T. Yoshino, Y. Suzuki and N. Kasagi, *J. Fluid Sci. Tech.*, **3**, 137 (2008)